Published OnlineFirst August 11, 2009; DOI: 10.1158/0008-5472.CAN-09-0540

Paclitaxel Directly Binds to Bcl-2 and Functionally Mimics Activity of Nur77

Cristiano Ferlini,[1] Lucia Cicchillitti,[2] Giuseppina Raspaglio,[1] Silvia Bartollino,[2] Samanta Cimitan,[3] Carlo Bertucci,[3] Simona Mozzetti,[1] Daniela Gallo,[1] Marco Persico,[4] Caterina Fattorusso,[4] Giuseppe Campiani,[5] and Giovanni Scambia[1]

[1]Laboratory of Antineoplastic Pharmacology, Department of Obstetrics and Gynecology, Catholic University of the Sacred Heart, Rome, Italy; [2]Department of Oncology, Catholic University of the Sacred Heart, Campobasso, Italy; [3]Department of Pharmaceutical Sciences, University of Bologna, Bologna, Italy; [4]Department of Natural Products, University of Napoli Federico II, Napoli, Italy; and [5]NatSynDrugs, Department of Chemistry, University of Siena, Siena, Italy

Abstract

We reported previously that Bcl-2 is paradoxically down-regulated in paclitaxel-resistant cancer cells. We reveal here that paclitaxel directly targets Bcl-2 in the loop domain, thereby facilitating the initiation of apoptosis. Molecular modeling revealed an extraordinary similarity between the paclitaxel binding sites in Bcl-2 and β-tubulin, leading us to speculate that paclitaxel could be mimetic of an endogenous peptide ligand, which binds both proteins. We tested the hypothesis that paclitaxel mimics Nur77, which, like paclitaxel, changes the function of Bcl-2. This premise was confirmed by Nur77 interacting with both paclitaxel targets (Bcl-2 and β-tubulin) and a peptide sequence mimicking the Nur77 structural region, thus reproducing the paclitaxel-like effects of tubulin polymerization and opening the permeability transition pore channel in mitochondria. This discovery could help in the development of novel anticancer agents with nontaxane skeleton as well as in identifying the clinical subsets responsive to paclitaxel-based therapy. [Cancer Res 2009;69(17):6906–14]

Introduction

Taxanes are known to target microtubules, interacting with β-tubulin (1) and thereby interfering with microtubule dynamics. Treatment with paclitaxel blocks the cell cycle at the transition from the metaphase to the anaphase (2) and then activates the intrinsic mitochondrial apoptotic pathway, as shown by the reduction in the mitochondrial membrane potential, followed by the opening of the permeability transition pore channel (PTPC). The subsequent release of proapoptotic factors, such as cytochrome *c* and apoptosis-inducing factor, leads to the activation of effector caspases and ultimately to apoptosis (reviewed in ref. 3). However, the exact molecular pathways connecting interference with microtubule dynamics to the activation of cell death remain unclear.

Nur77 (NGFI-B, TR3, NR4A1) is an orphan nuclear receptor induced by various stimuli such as growth promotion and stress. Translocation of Nur77 from the nucleus to the mitochondrial membrane represents a potent cell death signal (4). Lin and colleagues have shown that translocation of Nur77 to the mitochondrial membrane changes the function of Bcl-2 from a protector to a cell killer through a direct interaction with its disordered loop (5). Bcl-2 represents a member of the antiapoptotic factors in the Bcl family. It is often overexpressed in human cancers, particularly follicular B-cell lymphoma. Bcl-2 acts physiologically as a proton-efflux pump that prevents conductivity of the PTPC (6). Therefore, Bcl-2 participates in the regulation of the PTPC and acts as a gatekeeper that decreases the sensitivity to apoptotic stimuli (7). In 1999, Rodi and colleagues (8) used a library of phage-displayed peptides to show that Bcl-2 could be directly targeted by paclitaxel. More recently, we found that Bcl-2 was down-regulated in paclitaxel-resistant cells and tumor specimens (9), this being a paradox because normally antiapoptotic factors are overexpressed in drug-resistant cells.

The present work was aimed at assessing the hypothesis that paclitaxel mimics the binding motif of the Bcl-2 endogenous ligand Nur77, thereby making Bcl-2 proapoptotic. The results confirmed such hypothesis and revealed that paclitaxel is able to mimic the death signal mediated by Nur77.

Materials and Methods

Flow cytometric assessment of mitochondrial transmembrane potential. Cell culture procedures have been elsewhere described (9). Mitochondria were freshly isolated and mitochondrial transmembrane potential ($\Delta\Psi_m$) was assessed as described previously (10) using rhodamine 123 (Molecular Probes) and a FACScan flow cytometer.

Animal study. Female athymic mice were obtained from Charles River. Cells were s.c. injected into the right flank; after tumors grew to a size of 70 to 100 mg, mice were treated with 20 mg/kg/d paclitaxel, every third or fourth day × 4, via the i.v. route. Paclitaxel was dissolved in ethanol/Cremophor and diluted with physiologic saline to give required concentration. Treated animals were observed up to 2 months after paclitaxel treatment and were sacrificed when tumor weight was >10% of their body weight. After this period, surviving animals without sign of tumor regrowth were considered cured by treatment. Local ethics committee approved the project.

Western blot and immunoprecipitation experiments. Cells harvested in cold PBS were extracted in lysis buffer and immunoprecipitation was done as described previously (9). Antibodies were anti-Bcl-2 [N19 (Santa Cruz Biotechnology), clone 124 (DAKO), and BH3 (Abgent)], anti-Nur77 (Imgenex), anti-β-tubulin (H235; Santa Cruz Biotechnology), anti-class III β-tubulin polyclonal antibody (Covance), and isotype-matched nonimmune IgG (Sigma). Immunoprecipitation experiments were done in fresh cell lysates and paclitaxel incubation lasted 2 h at 4°C. Western blots were done as described previously (9).

DNA constructs. Human full-length Bcl-2 was obtained from lymphocytes by PCR with Pfu Taq polymerase (Promega) and *Hin*dIII/*Xba*I-cloned into pUSE (Upstate Biotechnology). A construct (pUSE-Bcl2Δ) was made in

Note: Supplementary data for this article are available at Cancer Research Online (http://cancerres.aacrjournals.org/).

Requests for reprints: Cristiano Ferlini, Laboratory of Antineoplastic Pharmacology, Department of Obstetrics and Gynecology, Catholic University of the Sacred Heart, L.go A. Gemelli 8, Rome, Italy 00168. Phone: 39-635502407; Fax: 39-635508736; E-mail: cferlini@rm.unicatt.it.

doi:10.1158/0008-5472.CAN-09-0540

Published OnlineFirst August 11, 2009; DOI: 10.1158/0008-5472.CAN-09-0540

which 49 amino acids (32-80) were deleted by inverse PCR and replaced with a linker of 4 alanines. The construct pUSE-Bcl2Pro^{39}Gly was obtained in the same way using the following primers: forward 5′-CCGGGGG-CCGCCCCCGCACCGGGCA-3′ and reverse 5′-ACCCGCGGCGCCCA-CATCTCCCGCATC-3′. Human Nur77 was obtained by PCR from human testis cDNA library (ResGen) with Pfu Taq polymerase (Promega). The PCR product was cloned into the *Bam*HI and *Eco*RI site of pUSE. The PCR product was then isolated after the *Bam*HI and *Eco*RI digestion and subsequently cloned into pQE1 (Qiagen). Nur77 fragments were prepared as described in ref. 5.

Far Western blotting. Bcl-2/Nur77 protein interaction was assessed by far Western blotting technique as described in Wu and colleagues (11). Briefly, 5 μg of Bcl-2 and carbonic anhydrase were blotted onto polyvinylidene difluoride membrane. Proteins were subjected to a denaturation process in protein binding buffer [100 mmol/L NaCl, 20 mmol/L Tris (pH 7.6), 0.5 mmol/L EDTA, 10% glycerol, 0.1% Tween 20, 2% milk powder, and 1 mmol/L DTT] containing decreasing amounts of guanidine-HCl from 6 to 0.1 mol/L. Renaturation of proteins was done overnight at 4°C in protein binding buffer without guanidine-HCl. Membranes were blocked with 5% milk in PBST (PBS with 0.05% Tween 20) for 2 h at 22°C. Drugs and bait proteins were added to protein binding buffer and membranes were incubated 16 h at 4°C. Membranes were washed three times in PBST and incubated with primary (anti-bait protein) and secondary (horseradish-conjugated) antibodies in PBST with 5% milk. Detection was done by Versadoc (Bio-Rad) after incubation in SuperSignal (Pierce). Quantitative densitometric analysis of the band of interest was done with the Phoretix software.

Biosensor experiments and proteins. Interaction analyses were done using a Biacore T100 (GE Healthcare). Sensor chips, *N*-ethyl-*N*′-hydroxysuccinimide, *N*-ethyl-*N*′-(3-dimethylaminopropyl) carbodiimmide, and ethanolamine HC were from GE Healthcare. Carbonic anhydrase, DMSO, furosemide, and other reagents were purchased from Sigma. Tubulin

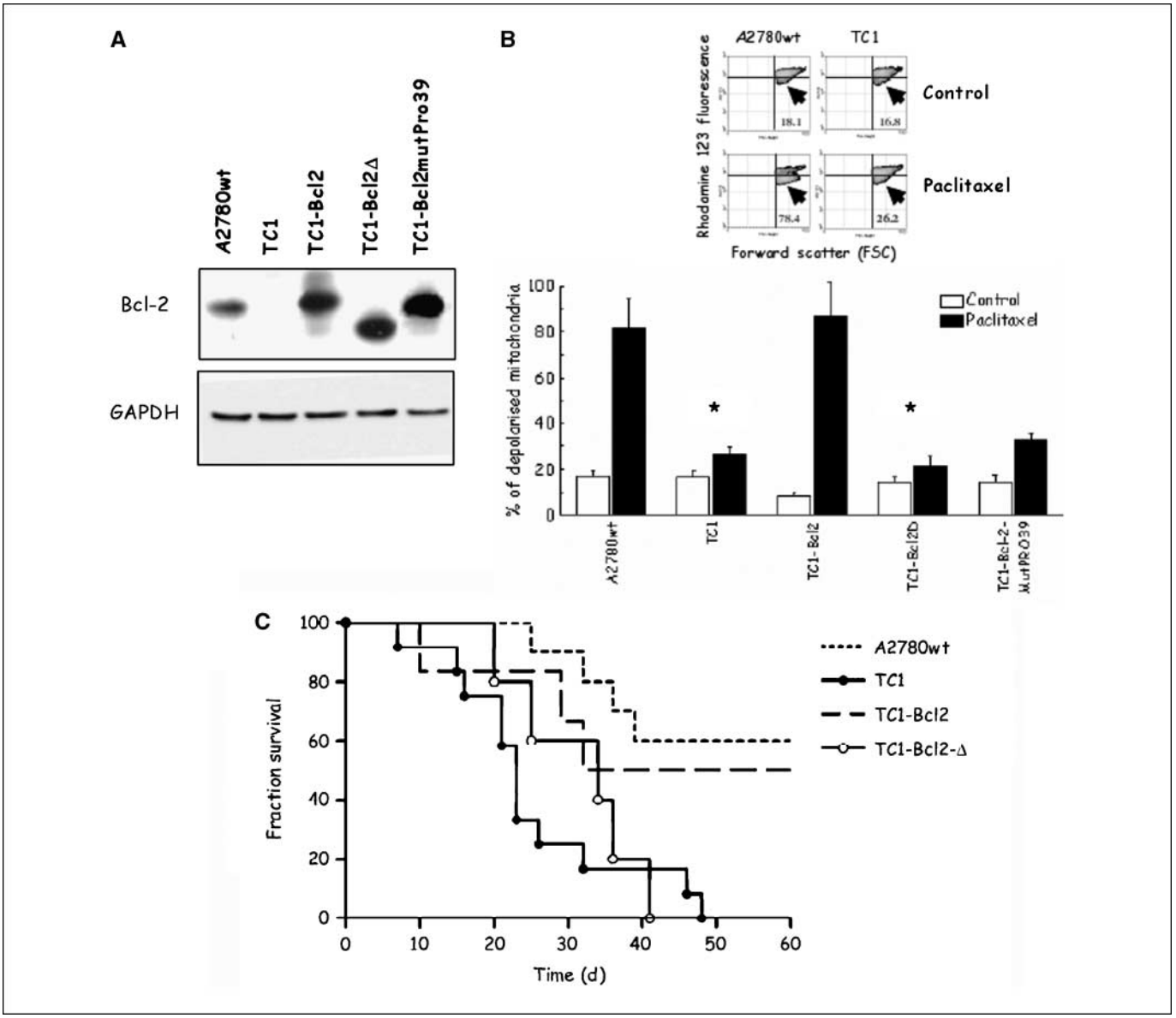

Figure 1. *A,* Western blot showing Bcl-2 expression in mitochondrial extracts. *Bottom,* glyceraldehyde-3-phosphate dehydrogenase (*GAPDH*) as the loading control. *B,* analysis of $\Delta\Psi_m$ in isolated mitochondria with or without treatment with paclitaxel (10 μmol/L). *Insets,* contour plots showing (*arrows*) the mitochondria in which the opening of PTPC induces the loss of $\Delta\psi_m$. *Columns,* mean of triplicate samples; *bars,* SD. *White* and *black columns,* control and paclitaxel-treated mitochondria. *, $P < 0.01$, statistically significant change with respect to the control. *C,* Kaplan-Meier plot showing the tumor progression of female athymic mice xenotransplanted with A2780, TC1, TC1-Bcl-2Δ, and TC1-Bcl2 cells. Animals were treated with paclitaxel 20 mg/kg/d every third or fourth day × 4.

Published OnlineFirst August 11, 2009; DOI: 10.1158/0008-5472.CAN-09-0540

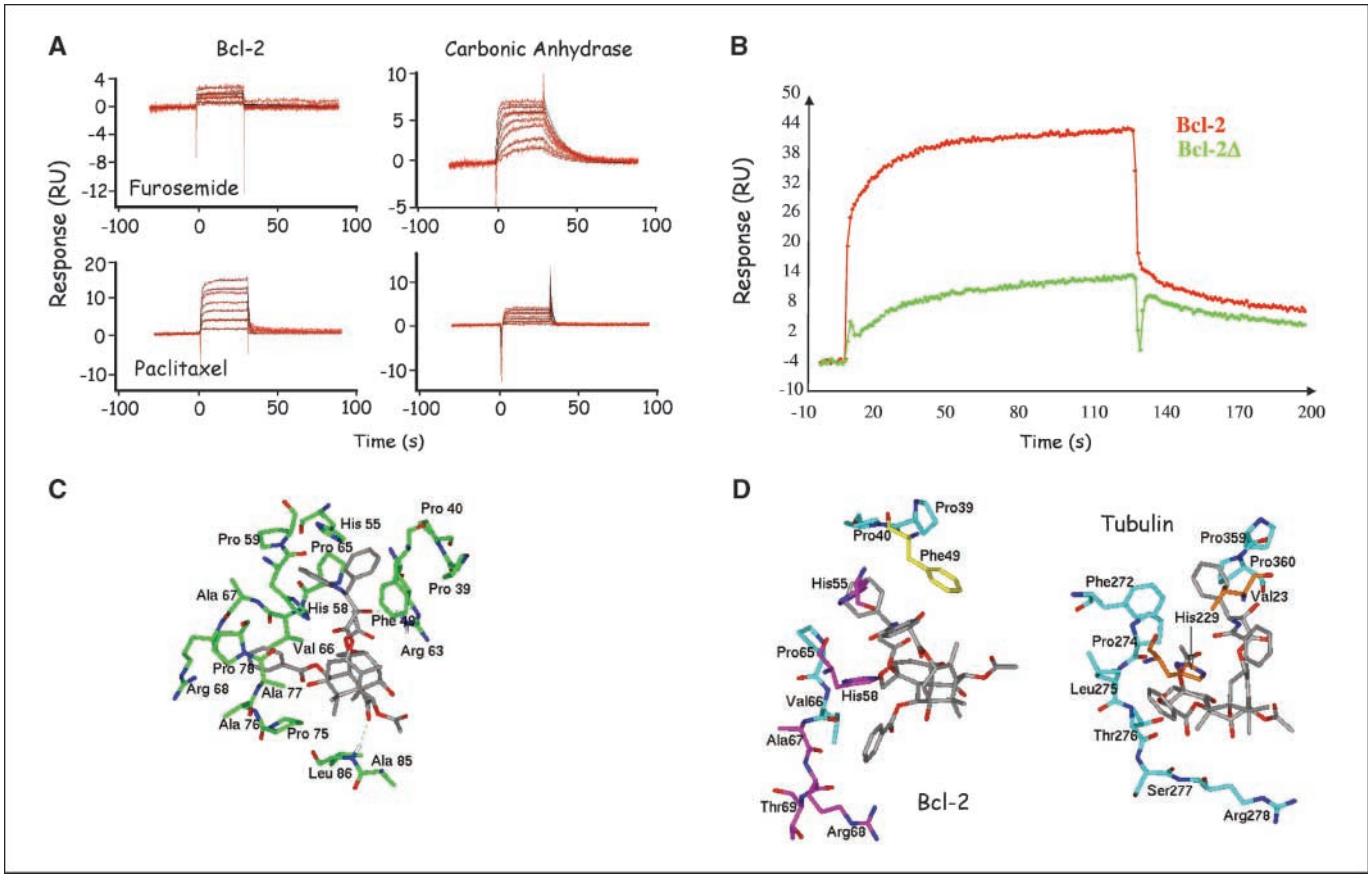

Figure 2. *A,* representative biosensograms of kinetic analysis of paclitaxel and furosemide against Bcl-2 and carbonic anhydrase. *B,* representative biosensogram of paclitaxel binding (10 μmol/L) in biochips with immobilized Bcl-2 (*red line*) or Bcl-2Δ (*green line*). *C,* paclitaxel docked into the Bcl-2 loop domain. *Capped sticks,* paclitaxel (*white*) and Bcl-2 residues (*green*) establishing hydrophobic interactions. *D,* comparison between paclitaxel binding site in Bcl-2 and β-tubulin. Proteins motifs involved in these binding sites are evidenced. *Magenta,* carbons of the WW domain ligand; *cyan,* carbons of the polyproline domain; *orange,* carbons of the LxxLL motif; *yellow,* carbons of Phe[49]. Structures were oriented to maximize binding site similarities. *RU,* response units.

preparations were from Cytoskeleton. Before starting the experiments, 10× PBS stock solution [1× = 137 mmol/L NaCl, 10 mmol/L phosphate, 2.7 mmol/L KCl (pH 7.4)] was prepared. Carbonic anhydrase at final concentration of 20 μg/mL was dissolved in 400 μL of 10 mmol/L sodium acetate (pH 5.0) after the biosensor was primed with immobilization buffer and equilibrated to 25°C. Surface of flow cell 4 was activated for 7 min using a mixture of 0.1 mol/L *N*-ethyl-*N*′-hydroxysuccinimide and 0.4 mol/L *N*-ethyl-*N*′-(3-dimethylaminopropyl) carbodiimmide. Carbonic anhydrase was injected until the target level of 1,500 response units was reached. For all the experiments, we chose flow cell 3 as unmodified reference surface. For immobilization of Bcl-2 and Bcl-2Δ, the sensor chip was equilibrated with PBS and then activated by injecting 0.2 mol/L *N*-ethyl-*N*′-hydroxysuccinimide/*N*-ethyl-*N*′-(3-dimethylaminopropyl) carbodiimmide followed by 5 to 10 μg injection of appropriate ligand in 10 mmol/L acetate at the correct pH according to the scouting procedure (pH 5.0 and 4.0 for Bcl-2 and Bcl-2Δ, respectively). After immobilization, 30 μL of regeneration buffer [4 mol/L guanidine HCl (pH 4.0)] were injected to remove noncovalently bound proteins. An initial series of buffer blanks was injected first to equilibrate fully the system. Finally, analyte was injected from lowest to highest concentrations using two blank injections and one concentration in duplicate. For immobilization of Nur77, the CM5 sensor chip was equilibrated with PBS and then activated by injecting 50 μL of 0.2 mol/L *N*-ethyl-*N*′-hydroxysuccinimide/*N*-ethyl-*N*′-(3-dimethylaminopropyl) carbodiimmide at 10 μL/min followed by 5 to 10 μg injection of appropriate ligand in 10 mmol/L acetate. Immobilization of Bcl-2 was done as described above. All analyses were done at 37°C, and for studying protein-protein interactions, kinetic data were obtained by diluting the samples in the running buffer PBS supplemented with P20 (0.05%). The surface was regenerated after each injection with 10 μL/min regeneration buffer. Tubulin polymerization experiments were described previously (12).

Computational modeling of Bcl-2. All molecular modeling studies were done on SGI Indigo II R10000 and SGI Octane 2XR10000 workstations. Molecular modeling was done using a combination of Monte Carlo and simulated annealing procedures. The generated models were then checked for quality using WHAT IF version WHATCHECK 7.0.5, which warranted the acceptability of the model. The linear functional motifs present in β-tubulin and Bcl-2 paclitaxel binding sites were identified by using the Eukaryotic Linear Motif server,[6] a resource for predicting small functional sites in eukaryotic proteins.

Results

Role of Bcl-2 as factor of drug resistance to paclitaxel. This study employed human ovary A2780 cancer cells and its paclitaxel-resistant counterpart TC1 (9). These cells, exhibiting Bcl-2 down-regulation, were stably transfected with a construct containing the full-length human BCL-2 gene (TC1-Bcl-2 cells) or a mutant with deletion of loop domain (amino acids 35-91; TC1-Bcl-2Δ), obtained as described by Chang and colleagues (13). The Bcl-2 mutant Pro[39]Gly was generated to abrogate functionally the loop. In fact, this mutation maps at the beginning of the loop in a critical region

[6] http://elm.eu.org/

Published OnlineFirst August 11, 2009; DOI: 10.1158/0008-5472.CAN-09-0540

part of a polyproline domain. This mutant was able to polymerize with Bcl-2 (14), with generation of dimers at low affinity. The binding affinity was comparable with those noticed with Bcl-2Δ, thereby supporting that the mutation $Pro^{39}Gly$ is similar to a functional abrogation of the loop (data not shown).

The expression levels of Bcl-2 obtained are depicted in Fig. 1*A*. Mitochondria were isolated and treated with paclitaxel at 10 μmol/L, which is the intracellular level achievable in patients (15). The status of $\Delta\Psi_m$ was monitored using rhodamine 123. Mitochondria in which PTPC is opened are recognizable for the loss of $\Delta\Psi_m$ and the decrease in rhodamine 123 fluorescence (Fig. 1*B*). In A2780 cells, paclitaxel treatment induced the loss of $\Delta\Psi_m$. In TC1 cells, with undetectable levels of Bcl-2, paclitaxel treatment only marginally increased the number of mitochondria in which $\Delta\Psi_m$ was reduced. In TC1-Bcl-2 cells, sensitivity to paclitaxel treatment was restored and mitochondria opened PTPC on paclitaxel treatment. Finally, in both mutants in which the loop was physically (TC1-Bcl-2Δ) or functionally (TC1-Bcl2Pro^{39}Gly) removed, the sensitivity to paclitaxel was abolished, with treatments having no effects on $\Delta\Psi_m$.

But does Bcl-2 play a role in the antitumor effect of paclitaxel? To address this issue, TC1 cells and its counterparts TC1-Bcl2 and TC1-Bcl-2Δ (Fig. 1*C*) were xenotransplanted in female athymic nude mice and the animals were treated with a paclitaxel regimen able to achieve a 50% cure rate in the parental A2780 model. Results showed the resistance of the TC1 model with no cures and 100% of tumor growth (A2780 versus TC1; $P < 0.001$). Similarly, there were no cures in TC1-Bcl-2Δ–treated animals showing only a slight delay in the onset of tumor growth (A2780 versus TC1-Bcl-2Δ; $P < 0.01$). The same regimen was able to produce in TC1-Bcl2 cells a 50% of cure, similarly to what obtained in A2780 (A2780 versus TC1-Bcl-2; P = nonsignificant), thereby showing that Bcl-2 status plays a pivotal role in the anticancer effects of paclitaxel.

Paclitaxel binds directly to the disordered loop of Bcl-2. Bcl-2 and Bcl-2Δ were immobilized on a biochip. We took advantage from the fact that Bcl-2 proteins, when properly folded, are capable to polymerize with other members of the Bcl-2 family. As negative control, we used Bcl-2 isolated in denaturizing conditions, which was always unable to generate polymers. Conversely, the recombinant proteins here used (Bcl-2wt, Bcl-2Δ, and Bcl2Pro^{39}Gly) were able to polymerize, thereby showing that they were properly folded and functionally active (data not shown). A biosensor was used to assess the ability of paclitaxel to bind Bcl-2 and Bcl-2Δ. As control, we immobilized in the parallel flow path carbonic anhydrase. The binding of paclitaxel was assessed on both targets (Bcl-2 and carbonic anhydrase), and the same was done with furosemide, a well-known binder of carbonic anhydrase (Fig. 2*A*). For Bcl-2, kinetic analysis revealed the binding with K_d value of 5.4 ± 3.1 μmol/L, whereas no binding was noticeable for furosemide. For carbonic anhydrase, no binding was detectable for paclitaxel and a K_d value of 2.9 ± 0.2 μmol/L for furosemide. Moreover, we immobilized on the two channels Bcl-2 and Bcl-2Δ. If a direct and specific paclitaxel-Bcl-2 binding interaction occurred, the paclitaxel-Bcl-2Δ interaction was not detectable (Fig. 2*B*). These findings show that paclitaxel binding site maps in the disordered loop of Bcl-2.

Molecular modeling of the interaction paclitaxel/Bcl-2. Paclitaxel was docked into the homology modeled NH_2-terminal loop of Bcl-2; during the calculation procedure, either paclitaxel or the Bcl-2 loop domain (amino acids 35-91) was left fully free. The resulting binding site is reported in Fig. 2*C*. The Bcl-2 loop forms a hydrophobic environment in which paclitaxel skeleton is embedded and which includes several aromatic residues (Phe^{49}, His^{55}, and His^{58}) that establish π-π interactions with the aromatic rings of the ligand and many aliphatic residues such as Pro^{65}, Val^{66}, Pro^{75}, Ala^{77}, and Pro^{78}. On the other hand, the side chains of Arg^{63} and the amide hydrogen of Leu^{86} are involved in hydrogen bonding to donor key groups of paclitaxel. The complete Bcl-2 paclitaxel binding site shows striking similarities with that of β-tubulin (16), with conserved amino acids including from Pro^{65} to Arg^{68} (Pro^{274}-Arg^{278} in β-tubulin), from Pro^{39} to Pro^{40} (Pro^{359}-Pro^{360} in β-tubulin), Phe^{49} (Phe^{272} in β-tubulin), His^{55} (Val^{23} in β-tubulin), and His^{58} (His^{229} in β-tubulin; Fig. 2*D*). Both paclitaxel binding sites contain a polyproline cleft together with several hydrophobic/aromatic residues. Polyproline-containing sequences were also found in a library of phage-displayed peptides that are able to bind paclitaxel (8), prompting us to investigate a possible role of paclitaxel as a peptidomimetic factor, capable of interfering with protein-protein interactions involving polyproline ligands. Accordingly, the ELM software (17) identified two SH3 domain ligands (72-78 and 85-91) and four WW domain ligands (53-58, 67-72, 71-76, and 84-89) in the human Bcl-2 loop. Analogously, a structural investigation of the paclitaxel binding site on β-tubulin provided evidence for the presence of two proline-rich domains (359-371

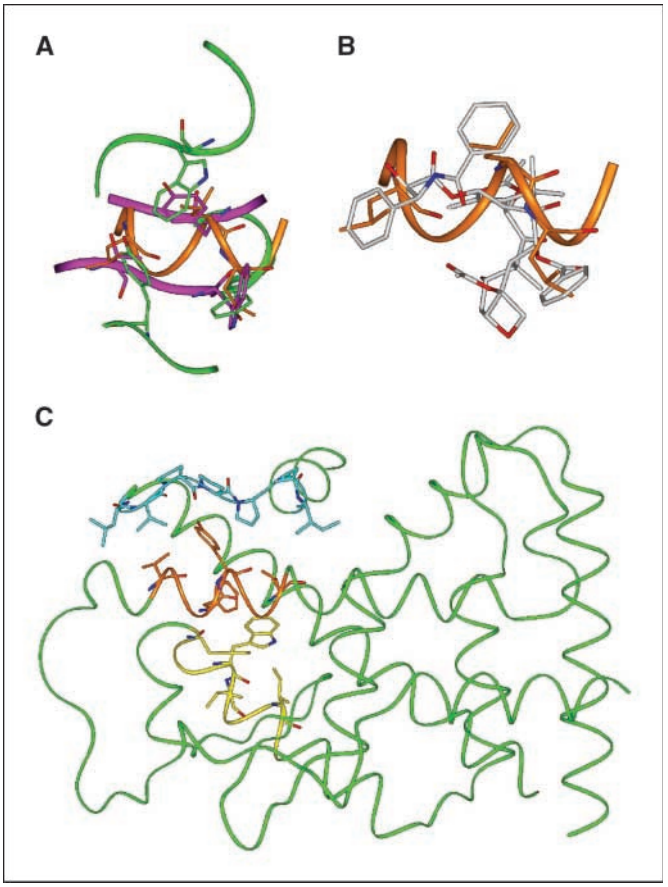

Figure 3. *A,* superimposition of interacting residues corresponding to WW (carbons in *magenta*), SH3 (carbons in *green*), and LxxLL (carbons in *orange*) domains. *Stick,* interacting residues; *red,* oxygen; *blue,* nitrogen. *B,* superimposition between paclitaxel (carbons in *white*) and LxxLL motif interacting residues (carbons in *orange*). *C,* overall view of the COOH-terminal of Nur77. Polyproline segment (Leu^{580}-Val^{587}, carbons in *cyan*) and LxxLL-like motif interacting residues (Val^{402}- Leu^{409}, carbons in *orange*; Phe^{478}-Leu^{486}, carbons in *yellow*).

Published OnlineFirst August 11, 2009; DOI: 10.1158/0008-5472.CAN-09-0540

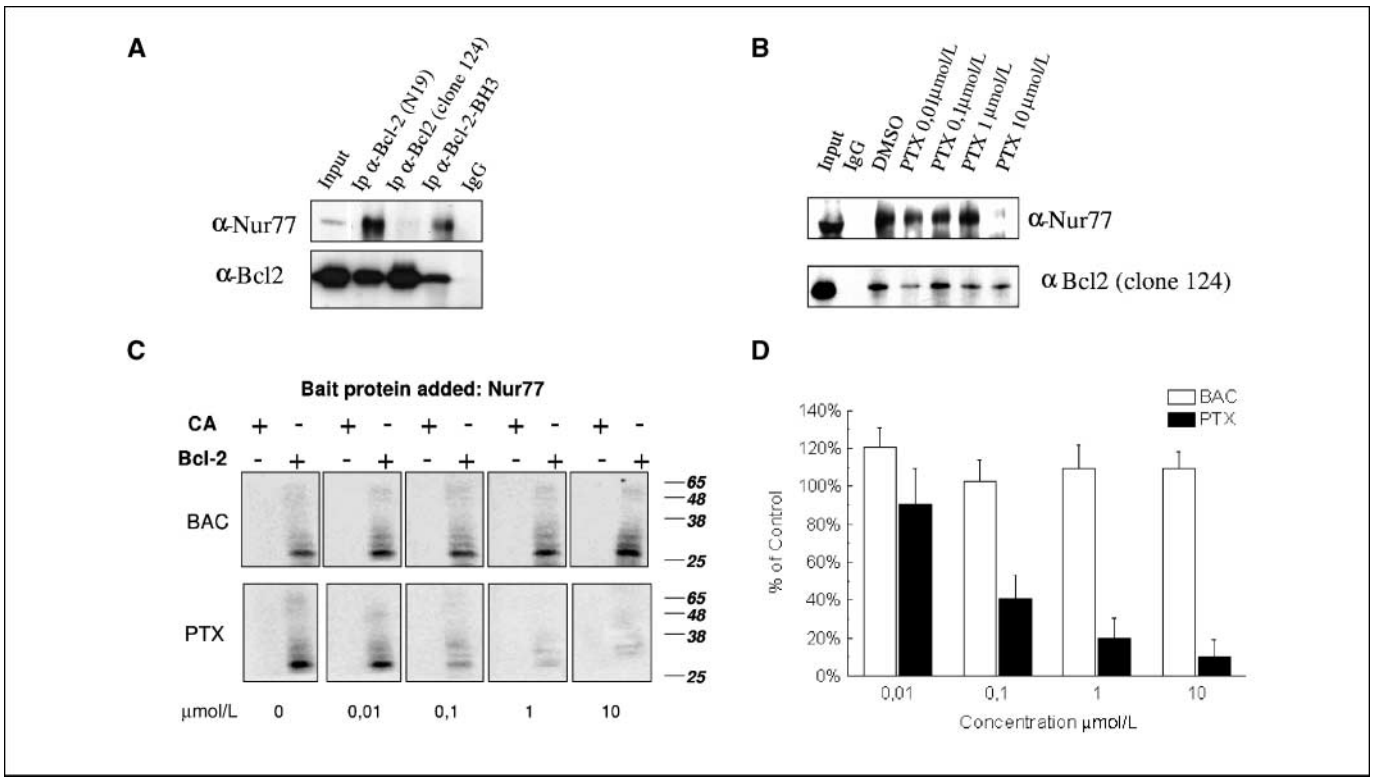

Figure 4. *A,* coimmunoprecipitation of Nur77 with Bcl-2 with a panel of anti-Bcl-2 antibodies. *B,* coimmunoprecipitation of Nur77 with Bcl-2 in the presence of increasing concentration of paclitaxel (*PTX*). *C,* representative far Western blot to detect the Nur77/Bcl-2 interaction and competition with 10-deacetyl baccatin III (*BAC*) and paclitaxel. Carbonic anhydrase (*CA*) served as negative control. *D,* bar chart summarizing the results of triplicate far Western blots. *Columns,* mean of three experiments; *bars,* SD. Data were obtained through densitometric analysis of the 27 kDa band.

and 272-278) and two LxxLL-like motif (20-28 and 227-231). We therefore investigated the molecular interactions among SH3, WW, and LxxLL domains and their ligands by analyzing several X-ray structures (Supplementary Table SI). SH3 and WW domains share common structural features: these structural features are similar to those displayed by the LxxLL motif, in which the first and the last Leu residues (i, i + 4; α helix) are structured like the interacting residues Thr and Trp i + 2 (i, i + 2; β-strand) in the WW domain (Fig. 3*A*), in agreement with a recent report (18) that the distance among C_α atoms of residues i and i + 4 on one face of an α helix is similar to the distance among C_α atoms of residues i and i + 2 along one strand of a β-hairpin.

We calculated the structural features of paclitaxel in its β-tubulin bound conformation; the results are reported in Supplementary Table SII. There is a striking similarity among the distances of the paclitaxel "side chains" (I-II, I-III, and II-III in Supplementary Table SII) and those of interacting residues in the SH3, LxxLL, and WW domains. Moreover, the paclitaxel skeleton includes a turn-like structure around bonds C3-C8 and C8-C9 that is compatible with both a type I-α_{RS} α turn and a type I-III β turn (Supplementary Table SII). Thus, paclitaxel skeleton resembles an α helix/β turn structure in which rings II, III, and I represent the side chains of residues i and i + 4 or i and i + 2 of α helix and β turn, respectively (Fig. 3*B*), thus mimicking a LxxLL-like protein domain. Accordingly, the three aromatic moieties of paclitaxel are engaged in hydrophobic contacts with similarly oriented hydrophobic residues both in the β-tubulin binding site (His^{229}, Val^{23}, and Phe^{272}) and in our Bcl-2 docked structure (His^{58}, His^{55}, and Phe^{49}), resembling LxxLL domain interactions. The oxetane ring of paclitaxel mimics a proline residue, and it is engaged in hydrophobic interactions in both β-tubulin (Pro^{274} and Leu^{275}) and Bcl-2 (Pro^{65} and Val^{66}), similarly to that observed for SH3 domain ligands. However, it remains a main difference in the Bcl-2 model, because there is no H-bond partner resembling the interaction between Thr^{276} of β-tubulin and paclitaxel. Despite this difference, homology is impressive and supports the hypothesis that paclitaxel mimics LxxLL-like and polyproline motifs in both targets (Bcl-2 and β-tubulin). About paclitaxel conformers available in literature (19, 20), all fitted into the model, but the best fit was obtained with the T-Taxol conformation (Supplementary Table SIII).

Peptide mimicry of paclitaxel. To characterize the interaction Nur77/Bcl-2, a panel of anti-Bcl-2 antibodies was used. Antibodies directed toward the NH_2 terminus and the BH3 domains were able to immunoprecipitate the Bcl-2-Nur77 complex, whereas the antibody with the epitope within the disordered loop (clone 124) did not (Fig. 4*A*). This result suggests that, as for paclitaxel, the disordered loop of Bcl-2 is responsible for Nur77 binding (5). To assess whether paclitaxel was able to interfere with the Bcl-2-Nur77 complex, whole-cell lysates from A2780 cells were treated with paclitaxel at concentrations up to 10 μmol/L, and coimmunoprecipitation experiments were done. As shown in Fig. 4*B*, 10 μmol/L paclitaxel was able to displace Nur77 from Bcl-2, suggesting that both paclitaxel and Nur77 target the same site on Bcl-2. To strengthen this result, the technique of far Western blot was used. Recombinant Bcl-2 was blotted into a membrane. After a process of renaturation with a gradient of guanidine-HCl, the protein was incubated with recombinant Nur77. After extensive washings, the complexes between the two proteins were detected with anti-Nur77

Published OnlineFirst August 11, 2009; DOI: 10.1158/0008-5472.CAN-09-0540

and Western blot. As expected, the interaction of the two proteins was detectable with a prominent band corresponding to the 27 kDa of Bcl-2 (Fig. 4*C*). The negative control of such experiments was represented by carbonic anhydrase, which was blotted in parallel with Bcl-2 and was unable to form complexes with Nur77 (Fig. 4*C*). Thereafter, competition experiments were done comparing paclitaxel with equimolar doses of 10-deacetyl baccatin III, which is without significant anticancer effects (21). Although no changes in the interaction Bcl-2/Nur77 were induced by 10-deacetyl baccatin III, paclitaxel clearly competed for the same binding site of Nur77, thereby revealing that paclitaxel and Nur77 have overlapping targets on Bcl-2 (Fig. 4*C* and *D*). There was an apparent discrepancy between the ability of paclitaxel to displace the interaction Bcl-2/Nur77 when analyzed with coimmunoprecipitation (effect at 10 μmol/L) and far Western blotting technique (effect at 0.1 μmol/L). It is likely that the discrepancy stems from the fact that, in the first case, paclitaxel will bind to both Bcl-2 and β-tubulin, thereby making paclitaxel less available for displacement of the complex Bcl-2/Nur77, whereas, in the second case, paclitaxel will bind only to Bcl-2, making the drug entirely available for the displacement.

Because the major target of paclitaxel is β-tubulin, we wanted to determine whether Nur77 was able to interact with this protein. Our results show that Nur77 coimmunoprecipitates with β-tubulin (Fig. 5*A*). To assess whether Nur77 induces the same phenotypic effects of paclitaxel in microtubules, we assessed class III β-tubulin (TUBB3) in A2780 and TC1 cells, and the counterparts stably transfected with Nur77, because paclitaxel enhances expression of this protein at the gene and protein levels (22). TUBB3 was up-regulated in A2780Nur77 cells compared with untransfected cells, with the same mobility shift observed in paclitaxel-resistant cell lines. In TC1 cells, which were chronically exposed to paclitaxel to maintain the resistant phenotype, TUBB3 was overexpressed and no further increase was detectable in TC1Nur77. Real-time PCR analysis confirmed that this up-regulation occurs at the gene level and that its extent in A2780Nur77 cells is similar to that in TC1 cells. This finding shows that Nur77 exerts paclitaxel-like effects on microtubules.

To characterize the interactions between Nur77 and Bcl-2/tubulin, we performed experiments using either Bcl-2 or tubulin as the ligand on the chip and using recombinant Nur77 as the analyte. The Nur77-Bcl-2 binding was characterized by very low K_d value ($3 \pm 1.4 \times 10^{-11}$ mol/L), whereas the interaction of Nur77 with tubulin was 3 orders of magnitude weaker ($4 \pm 0.5 \times 10^{-8}$ mol/L; Fig. 5*C* and *D*).

Therefore, we analyzed the COOH-terminal fragment of Nur77 (Fig. 3*C*), which reportedly interacts strongly with Bcl-2 (5). This region includes a COOH-terminal polyproline segment (580-586) interacting with three hydrophobic residues (Val^{402}, Phe^{405}, and Tyr^{406}), and its structural comparison with SH3 domains in complexes with polyproline ligands revealed the same orientation of the interacting residues. Moreover, residues Phe^{405} and Tyr^{406}

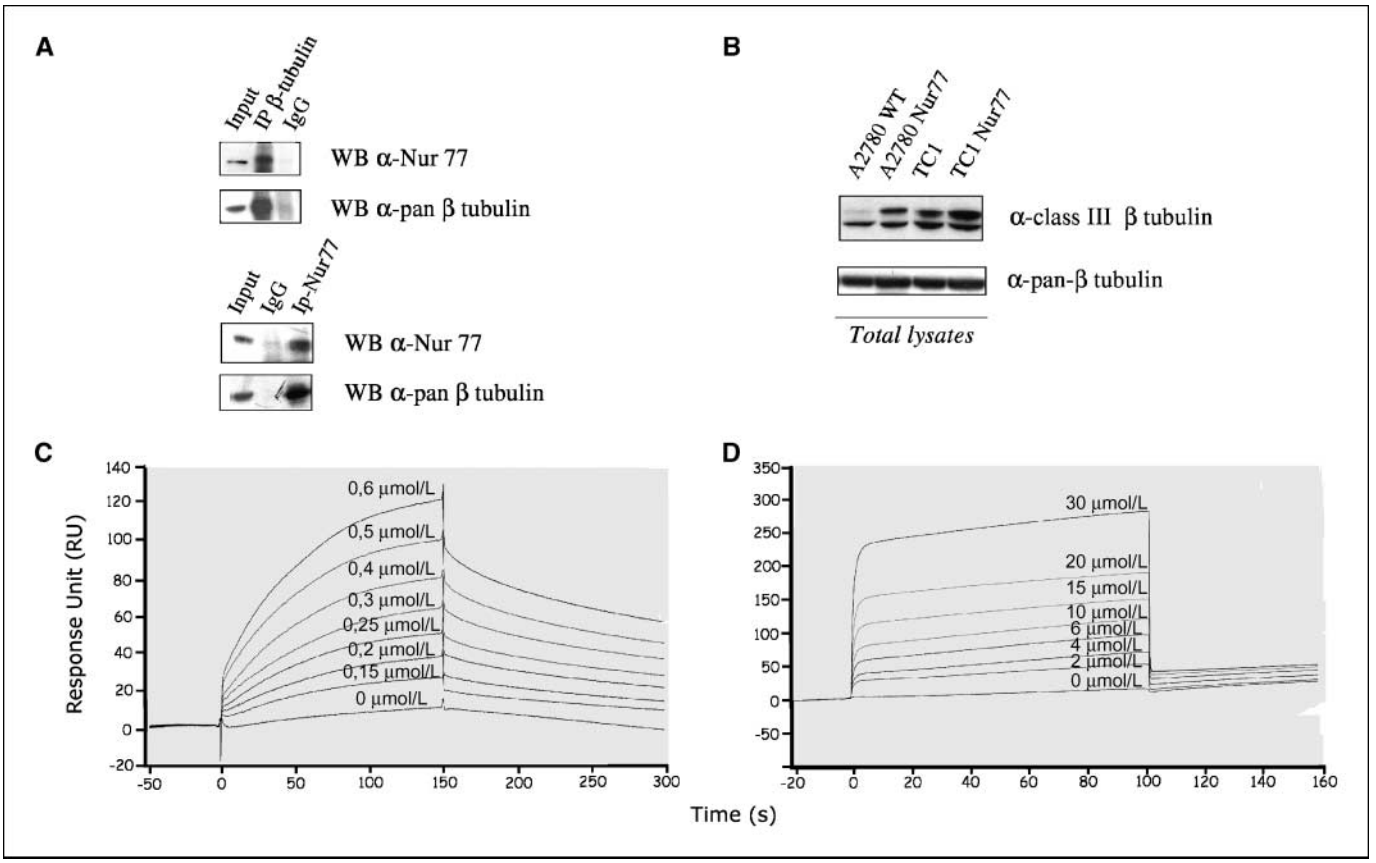

Figure 5. *A,* coimmunoprecipitation in whole-cell lysates of A2780 of Nur77 with β-tubulin. *B,* Western blot analysis of class III β-tubulin. Two bands were detectable. The top band is related to the cytoskeletal TUBB3, whereas the bottom band, constitutively expressed and not up-regulated in paclitaxel-resistant cells, is relative to mitochondrial TUBB3 (36). *C,* biosensogram for the interaction Bcl-2/Nur77 and Nur77/tubulin. Nur77 and Bcl-2 were analyte and ligand, respectively. *D,* Nur77 and tubulin were ligand and analyte, respectively. Each curve corresponds to a single analyte concentration.

Published OnlineFirst August 11, 2009; DOI: 10.1158/0008-5472.CAN-09-0540

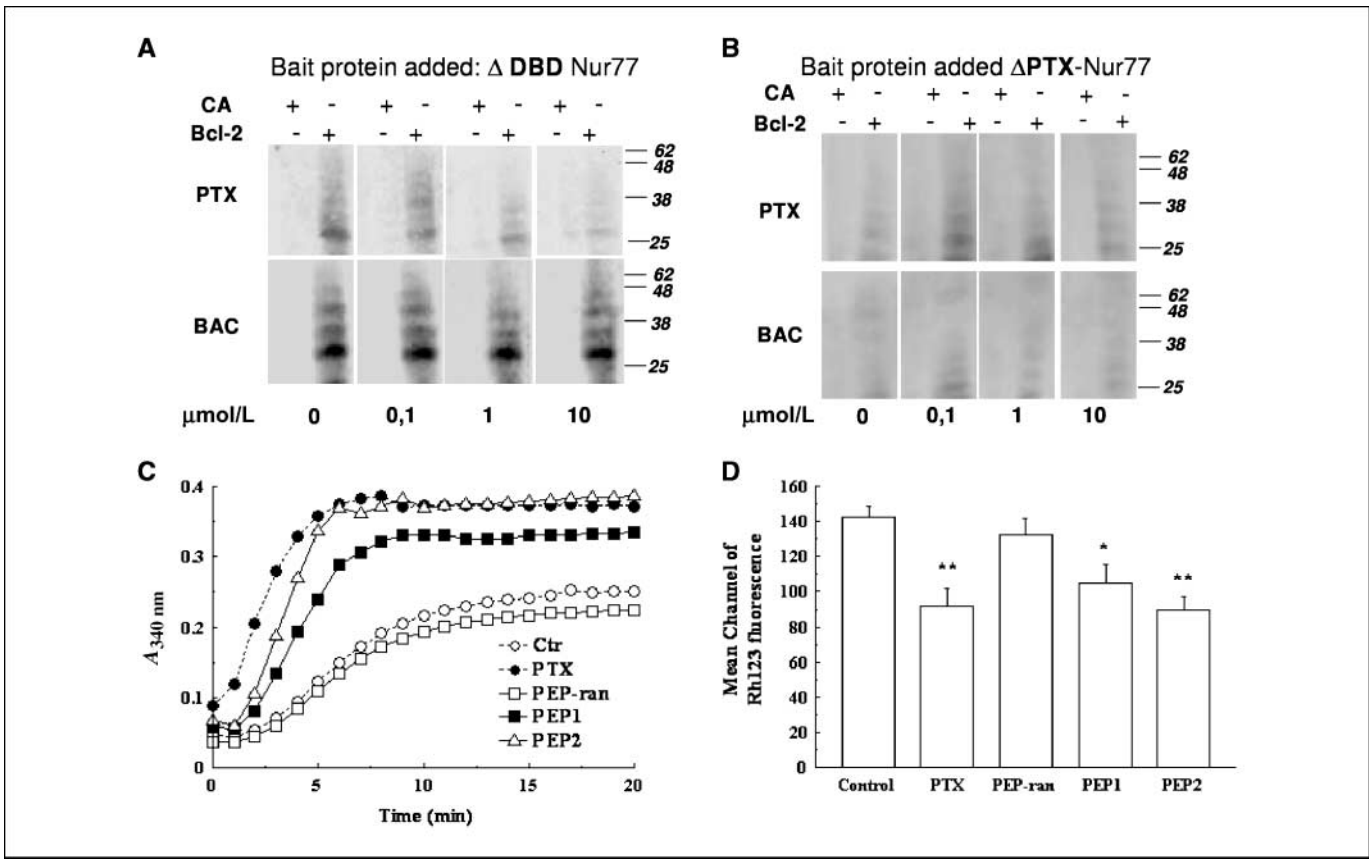

Figure 6. Representative far Western blot of the interaction Nur77ΔDBD/Bcl-2 (*A*) or Nur77ΔPTXD/Bcl-2 (*B*) and paclitaxel or 10-deacetyl baccatin III competition. Carbonic anhydrase served as negative control. *C,* line chart showing tubulin oligomerization experiments with control, paclitaxel, PEP1, PEP2, and PEP-ran. Triplicate experiments were done at 37°C with 0.8 mg of MAP-containing tubulin for each condition. Compounds were used at 10 μmol/L. *D,* bar chart summarizing mitochondrial effects of the peptides. *Columns,* mean of triplicate samples; *bars,* SD. *, $P = 0.05$; **, $P = 0.01$. *Rh123,* rhodamine 123.

are located in the H3 helix of Nur77 within a sequence containing a repeated LxxLL-like motif (Val^{402}-Leu^{409}). In particular, Phe^{405} is also involved in π-π interactions with residues Phe^{478} and Trp^{481}, which are part of another LxxLL-like structure (H7 helix; Phe^{478}-Ile^{482}) in the hydrophobic core of the ligand-binding domain. Thus, the interaction of Nur77 with the Bcl-2 loop could be mediated through a LxxLL-like domain that could in turn be mimicked by paclitaxel as evidenced in Fig. 3*B*.

To enforce the modeling data, we prepared two Nur77 mutants. The first one was featured by deletion of the DNA-binding domain (amino acids 1-325, Nur77ΔDBD) and the second one with deletion of the paclitaxel mimicked domain described in Fig. 3*C* (amino acids 466-590, Nur77ΔPTXD). With these mutants, we performed far Western blotting as above described. If with Nur77ΔDBD there was binding of Nur77 to Bcl-2 and competition with paclitaxel (Fig. 6*A*), no binding and competition were noticed with the Nur77ΔPTXD (Fig. 6*B*). These observations prompted us to design a peptide reproducing the Nur77 region mimicked by paclitaxel. We designed two peptides, LVPPPPIVGYF (PEP1) and LVPPPPIVPYF (PEP2), corresponding to the sequences 580-587 (Fig. 3*C, cyan*) and 406-405 (Fig. 3*C, orange*) of NUR77, spaced with G and P as linkers for PEP1 and PEP2, respectively. A control peptide was used with the common components of PEP1 and PEP2 but in a random sequence (PLIPVYPFVP; PEP-ran). In tubulin oligomerization experiments (Fig. 6*C* and *D*), the effect of PEP2 superposed that of paclitaxel, whereas that of PEP1 was slightly lower. PEP-ran did not vary the kinetics of microtubule assembly. The same pattern of paclitaxel mimicry was evident at the mitochondrial level. PEP2 reduced $\Delta\Psi_m$ by an extent similar to that of paclitaxel, whereas that of PEP1 was again slightly lower. Analogously to the tubulin oligomerization experiments, PEP-ran did not vary $\Delta\Psi_m$. Collectively, these findings show that the biologic activities of paclitaxel can be mimicked by a peptide corresponding to the Bcl-2 binding motif of Nur77.

Discussion

Bcl-2 plays a pivotal role in protecting cells from death in hematopoietic systems, whereas in solid tumors its physiologic role is still unclear. In an elegant review, Brown and Attardi (23) reported how controversial is the role of Bcl-2 as mediator of drug and radioresistance. Furthermore, to our knowledge, no clinical evidence of a clear association between Bcl-2 up-regulation and chemoresistance has been reported in solid tumors (24). Instead, in several tissues, increased Bcl-2 expression has been related to drug responsiveness in cancers treated with taxane-including regimens such as breast (25) and prostate (26) cancers. Accordingly, early pivotal articles reported that paclitaxel activity is inhibited in the absence of Bcl-2 (27) or in the presence of a Bcl-2 mutant lacking the disordered loop domain (28). Here, we reported that Bcl-2 reexpression in paclitaxel-resistant TC1 cells xenotransplanted on nude athymic mice restored chemosensitivity to paclitaxel, thereby

enforcing the hypothesis that in solid tumors Bcl-2 is a factor of chemosensitivity to paclitaxel. But how does the drug play this role? Clearly, paclitaxel interacts with β-tubulin and disrupts the microtubule dynamics. However, along with this well-known activity, the drug induces a direct modulation of the mitochondrial function (15, 29, 30). Here we extend these previous reports and provide direct evidence that paclitaxel changes the function of Bcl-2 via a direct targeting of mitochondria. Bcl-2 acts as a gatekeeper of the PTPC (7) but, in the presence of paclitaxel, its function of blocking the PTPC is abolished and reversed, with it instead easing the opening of the channel and the consequent reduction in $\Delta\Psi_m$. This phenomenon underlies the paradox of paclitaxel-induced Bcl-2 down-regulation observed in paclitaxel-resistant tumor cells and cancer patients (9).

Once the potential binding site was identified in the disordered loop of Bcl-2, molecular modeling allowed us to characterize the homology between the experimentally defined paclitaxel binding site of β-tubulin (16) and the site modeled in Bcl-2. But why do cells contain at least two paclitaxel protein targets? Similarities suggest that paclitaxel is a peptidomimetic compound able to mimic the endogenous ligand of the paclitaxel binding proteins. This hypothesis was proposed by Leu and colleagues (31), who discovered that a monoclonal anti-idiotypic antibody generated against paclitaxel was able to simulate paclitaxel activity, thereby showing that a protein could mimic paclitaxel. Functionally, the mimicked motif delivers a potent death signal. Throughout evolution, many species have used similar strategies. In fact, albeit not chemically related, several natural compounds including epothilones and eleutherobins similarly interact with the paclitaxel binding site in β-tubulin. Recently, also the tat protein of HIV has been identified as a ligand for the paclitaxel binding site in tubulin, and this interaction appears to play a pivotal role in inducing apoptosis in HIV-infected T cells (32, 33). But which is the mimicked protein? Given the similarity, a good candidate could be Nur77, which, like paclitaxel, converts Bcl-2 from a protector to a killer (5). This hypothesis was assessed in our study by looking at the ability of Nur77 to interact with Bcl-2 and performing experiments aimed at detecting direct competition between paclitaxel and Nur77 for binding to Bcl-2. Moreover, we showed that Nur77 binds to β-tubulin, thereby again resembling the behavior of paclitaxel. Stable transformation with Nur77 leads to the overexpression of TUBB3, a phenomenon described previously in paclitaxel-resistant cells. This prompted us to analyze the structure of paclitaxel, which revealed that it is able to mimic a peptide containing both a LxxLL/SH3/WW-like domain and a polyproline domain. Thereafter, we extended this approach by designing the peptides PEP1 and PEP2, predicted to display the same biological activity of paclitaxel. The activity of the peptides confirmed our hypothesis that paclitaxel is a peptidomimetic compound bearing the same death signal that is delivered physiologically by Nur77, disruption of microtubule dynamics, and Bcl-2-mediated PTPC opening. In this context, the increased levels of TUBB3 in cells that stably overexpressed Nur77 suggest that TUBB3 provides a pathway for circumventing Nur77-dependent death signal. Unfortunately, the same pathway is activated in paclitaxel-treated patients, thereby explaining why TUBB3 is a marker of poor prognosis and drug resistance (34, 35).

Nature has done combinatorial chemistry for hundred million years. This led to the synthesis of paclitaxel and other agents sharing at least partly its pharmacophore, including the viral products of HIV-1, which are able to mimic the death message delivered by Nur77. This knowledge could be useful in designing novel strategies to manipulate this message, enhancing or inhibiting it as needed.

Disclosure of Potential Conflicts of Interest

No potential conflicts of interest were disclosed.

Acknowledgments

Received 2/13/09; revised 6/5/09; accepted 6/16/09; published OnlineFirst 8/11/09.

Grant support: Italian Ministry of University and Research Grant 4201011.

The costs of publication of this article were defrayed in part by the payment of page charges. This article must therefore be hereby marked *advertisement* in accordance with 18 U.S.C. Section 1734 solely to indicate this fact.

We thank Cristiana Gaggini and Federica Pignatelli for technical assistance.

References

1. Schiff PB, Fant J, Horwitz SB. Promotion of microtubule assembly *in vitro* by Taxol. Nature 1979;277:665–7.
2. Jordan MA, Toso RJ, Thrower D, Wilson L. Mechanism of mitotic block and inhibition of cell proliferation by Taxol at low concentrations. Proc Natl Acad Sci U S A 1993;90:9552–6.
3. Bhalla KN. Microtubule-targeted anticancer agents and apoptosis. Oncogene 2003;22:9075–86.
4. Li H, Kolluri SK, Gu J, et al. Cytochrome *c* release and apoptosis induced by mitochondrial targeting of nuclear orphan receptor TR3. Science 2000;289:1159–64.
5. Lin B, Kolluri SK, Lin F, et al. Conversion of Bcl-2 from protector to killer by interaction with nuclear orphan receptor Nur77/TR3. Cell 2004;116:527–40.
6. Shimizu S, Eguchi Y, Kamiike W, et al. Bcl-2 prevents apoptotic mitochondrial dysfunction by regulating proton flux. Proc Natl Acad Sci U S A 1998;95:1455–9.
7. Voehringer DW. BCL-2 and glutathione: alterations in cellular redox state that regulate apoptosis sensitivity. Free Radic Biol Med 1999;27:945–50.
8. Rodi DJ, Janes RW, Sanganee HJ, et al. Screening of a library of phage-displayed peptides identifies human bcl-2 as a Taxol-binding protein. J Mol Biol 1999;285:197–203.
9. Ferlini C, Raspaglio G, Mozzetti S, et al. Bcl-2 down-regulation is a novel mechanism of paclitaxel resistance. Mol Pharmacol 2003;64:51–8.
10. Ferlini C, Scambia G. Assay for apoptosis using the mitochondrial probes, rhodamine123 and 10-*N*-nonyl acridine orange. Nat Protoc 2007;2:3111–4.
11. Wu Y, Li Q, Chen XZ. Detecting protein-protein interactions by far Western blotting. Nat Protoc 2007;2:3278–84.
12. Ferlini C, Raspaglio G, Mozzetti S, et al. The seco-taxane IDN5390 is able to target class III β-tubulin and to overcome paclitaxel resistance. Cancer Res 2005;65:2397–405.
13. Chang BS, Minn AJ, Muchmore SW, Fesik SW, Thompson CB. Identification of a novel regulatory domain in Bcl-X(L) and Bcl-2. EMBO J 1997;16:968–77.
14. Mathura VS, Soman KV, Varma TK, Braun W. A multimeric model for murine anti-apoptotic protein Bcl-2 and structural insights for its regulation by post-translational modification. J Mol Model 2003;9:298–303.
15. Andre N, Braguer D, Brasseur G, et al. Paclitaxel induces release of cytochrome *c* from mitochondria isolated from human neuroblastoma cells. Cancer Res 2000;60:5349–53.
16. Lowe J, Li H, Downing KH, Nogales E. Refined structure of α β-tubulin at 3.5 A resolution. J Mol Biol 2001;313:1045–57.
17. Puntervoll P, Linding R, Gemund C, et al. ELM server: a new resource for investigating short functional sites in modular eukaryotic proteins. Nucleic Acids Res 2003;31:3625–30.
18. Fasan R, Dias RL, Moehle K, et al. Using a β-hairpin to mimic an α-helix: cyclic peptidomimetic inhibitors of the p53-2 protein-protein interaction. Angew Chem Int Ed Engl 2004;43:2109–12.
19. Snyder JP, Nettles JH, Cornett B, Downing KH, Nogales E. The binding conformation of Taxol in β-tubulin: a model based on electron crystallographic density. Proc Natl Acad Sci U S A 2001;98:5312–16.
20. Ganesh T, Guza RC, Bane S, et al. The bioactive Taxol conformation on β-tubulin: experimental evidence from highly active constrained analogs. Proc Natl Acad Sci U S A 2004;101:10006–11.
21. Battaglia A, Bernacki RJ, Bertucci C, et al. Synthesis and biological evaluation of 2′-methyl taxoids derived from baccatin III and 14β-OH-baccatin III 1,14-carbonate. J Med Chem 2003;46:4822–5.
22. Burkhart CA, Kavallaris M, Band HS. The role of β-tubulin isotypes in resistance to antimitotic drugs. Biochim Biophys Acta 2001;1471:O1–9.
23. Brown JM, Attardi LD. The role of apoptosis in cancer development and treatment response. Nat Rev Cancer 2005;5:231–7.
24. Brown JM, Wilson G. Apoptosis genes and resistance

Published OnlineFirst August 11, 2009; DOI: 10.1158/0008-5472.CAN-09-0540

to cancer therapy: what does the experimental and clinical data tell us? Cancer Biol Ther 2003;2:477–90.

25. Callagy GM, Pharoah PD, Pinder SE, et al. Bcl-2 is a prognostic marker in breast cancer independently of the Nottingham Prognostic Index. Clin Cancer Res 2006;12:2468–75.

26. Yoshino T, Shiina H, Urakami S, et al. Bcl-2 expression as a predictive marker of hormone-refractory prostate cancer treated with taxane-based chemotherapy. Clin Cancer Res 2006;12:6116–24.

27. Haldar S, Chintapalli J, Croce CM. Taxol induces bcl-2 phosphorylation and death of prostate cancer cells. Cancer Res 1996;56:1253–5.

28. Fang G, Chang BS, Kim CN, et al. "Loop" domain is necessary for Taxol-induced mobility shift and phosphorylation of Bcl-2 as well as for inhibiting Taxol-induced cytosolic accumulation of cytochrome *c* and apoptosis. Cancer Res 1998;58:3202–8.

29. Evtodienko YV, Teplova VV, Sidash SS, Ichas F, Mazat JP. Microtubule-active drugs suppress the closure of the permeability transition pore in tumour mitochondria. FEBS Lett 1996;393:86–8.

30. Esteve MA, Carre M, Braguer D. Microtubules in apoptosis induction: are they necessary? Curr Cancer Drug Targets 2007;7:713–29.

31. Leu JG, Chen BX, Diamanduros AW, Erlanger BF. Idiotypic mimicry and the assembly of a supramolecular structure: an anti-idiotypic antibody that mimics Taxol in its tubulin-microtubule interactions. Proc Natl Acad Sci U S A 1994;91:10690–4.

32. Chen D, Wang M, Zhou S, Zhou Q. HIV-1 Tat targets microtubules to induce apoptosis, a process promoted by the pro-apoptotic Bcl-2 relative Bim. EMBO J 2002;21:6801–10.

33. de Mareuil J, Carre M, Barbier P, et al. HIV-1 Tat protein enhances microtubule polymerization. Retrovirology 2005;2:5.

34. Mozzetti S, Ferlini C, Concolino P, et al. Class III β-tubulin overexpression is a prominent mechanism of paclitaxel resistance in ovarian cancer patients. Clin Cancer Res 2005;11:298–305.

35. Ferrandina G, Zannoni GF, Martinelli E, et al. Class III β-tubulin overexpression is a marker of poor clinical outcome in advanced ovarian cancer patients. Clin Cancer Res 2006;12:2774–9.

36. Cicchillitti L, Penci R, Di Michele M, et al. Proteomic characterization of cytoskeletal and mitochondrial class III β-tubulin. Mol Cancer Ther 2008;7:2070–9.

Cancer Research
The Journal of Cancer Research (1916–1930) | The American Journal of Cancer (1931–1940)

AACR American Association for Cancer Research

Paclitaxel Directly Binds to Bcl-2 and Functionally Mimics Activity of Nur77

Cristiano Ferlini, Lucia Cicchillitti, Giuseppina Raspaglio, et al.

Cancer Res 2009;69:6906-6914. Published OnlineFirst August 11, 2009.